

Analysis of CryoSat's radar altimeter waveforms over different Arctic sea ice regimes

MARTA ZYGMUNTOWSKA, KIRILL KHVOROSTOVSKY

Nansen Environmental and Remote Sensing Center

Abstract

Satellite altimetry has been used to derive information about sea ice thickness in the Arctic already for several decades. As part of the algorithms applied the shape of the radar signal is used to identify leads, the open water between ice floes. Analysis of airborne altimeter data reveals that the waveform shape can additionally be used to identify different sea ice types. In this study we analyze signal waveforms from ESA's CryoSat-2 satellite, to test the possibility of sea ice classification based on radar altimeter waveforms on an Arctic wide scale. We define six parameters to account for the difference in the shape of the radar waveforms obtained over First- and Multi-Year-Ice and find significant differences for several of these parameters. The Pulse Peakiness, Stack Standard Deviation and Leading Edge Width show the largest difference. These waveform parameters can thus be used to classify First- and Multi-Year-Ice over large areas of the Arctic Ocean. However, analyzing the spatial distribution we find some discrepancies compared to other retrievals of sea ice type. CryoSat waveform parameters have values typical for Multi-Year-Ice over large areas classified as First-Year-Ice. These areas are co-located with strong gradients in drift speed, indicating, that the radar signal is mainly sensitive to surface roughness. Potentially this information could be used to reduce biases in the freeboard retrievals and to improve estimates of sea ice thickness.

I. INTRODUCTION

Decline in sea ice thickness is one of the main indicators of climate change (Stocker et al., 2013), and radar altimetry is one of the main tools used to measure this decline (Giles et al., 2008; Laxon et al., 2013). Consequently in the last decade, many attempts have been made to improve the algorithms used to derive sea ice thickness from radar altimetry. Algorithms have to consider how to detect open water between ice floes (Laxon, 1994; Laxon et al., 2013; Armitage and Davidson, 2013), retrieve freeboard, and then convert these measurements into an estimate of sea ice thickness (Wadhams et al., 1992; Giles et al., 2007). Sea ice thickness is then assumed to be around 10 times the sea ice freeboard (Wadhams et al., 1992). With the launch of CryoSat-2 in 2010 (Drinkwater et al., 2004) a new generation of radar altimeters is utilized (Wingham et al., 2006). The synthetic aperture approach used for the SAR/Interferometric Radar ALtimeter (SIRAL) onboard CryoSat-2 enhances the resolution along track (Raney, 1998; Wingham et al., 2006) and thus provides more detailed information about the surface properties.

Already for conventional altimeters it is well known, that the returned signal waveforms are sensitive to surface properties (Fetterer, 1992). Over oceans it is thus a well established method to use the shape and strength of the signal to retrieve information about wave height or wind speed (e.g. Fedor and Brown, 1982; Gourrion et al., 2002). Over sea ice it has been found that the strongest return comes from leads (Fetterer, 1992) and the signal strength is decreasing from flat to ridged sea ice (Fedor et al., 1989). Ulander (1987) and Drinkwater (1991) additionally found a correlation between radar backscatter from SAR images and the radar altimeter signal strength and width. Even though these results indicated that a distinction between ice types is possible based on the shape of the radar altimeter signal waveform, the methods have not been developed any further for a long time. Just recently, encouraged by the new capabilities resulting from the SAR technique used for CryoSat-2, Zygmuntowska et al. (2013a) presented a classification method based on measurements from an airborne synthetic aperture radar altimeter. The method is able to distinguish between First- and Multi-Year-Ice, using only the characteristics of the radar altimeter signal waveforms. They were able to classify 80% of the waveforms correctly using a combination of different waveform characteristics and applying a Bayesian based approach.

For satellite-based altimeters there is so far no algorithm that is able to distinguish between different sea ice types. The current algorithms for Envisat and CryoSat-2 use the waveform shape only to distinguish between leads and ice floes (Laxon et al., 2003, 2013; Hendricks et al., 2013). However, for accurate retrieval of sea ice thickness from freeboard data, information about sea ice type is needed. The type of sea ice determines the snow and ice properties which can highly influence the estimates of sea ice thickness (Alexandrov et al., 2010; Zygmuntowska et al., 2013b). In this study we therefore analyze waveform characteristics over different sea ice regimes, to check if sea ice classification is possible based on signal waveforms from CryoSat's radar altimeter SIRAL. We analyze one winter of CryoSat-2 data over the entire Arctic ocean, and compare waveform characteristics to other retrievals of sea ice type.

This paper is outlined as follows: First we describe the CryoSat-2 data, and the parameters used to characterize the shape of the radar signal waveforms. We compare our results to other satellite retrievals of sea ice type and discuss the ice properties which influence the different instruments used. Finally we discuss the potential applications and limitations of this work.

II. DATA

In this section we describe the radar waveform parameters analyzed over different surface regimes in the Arctic. Additionally we describe different data sets used for comparison with our results, such as other ice type retrievals, and sea ice drift.

1. CryoSat-2 waveform parameters

The primary data set in this study is from ESA's CryoSat-2 satellite. CryoSat-2 was launched in 2010 and was ESA's first satellite mission specifically designed to measure changes in the Earth's cryosphere. The satellite orbit has an inclination of 92 degrees, and a repeat cycle of 369 days. Additional sub-cycles every 30 days enable to monitor the Arctic on a regular grid on a monthly basis. CryoSat's payload instrument, the SAR/Interferometric Radar Altimeter (SIRAL), operates with center frequency of 13.575 GHz and has a receiving bandwidth of 360 MHz. After processing the footprint size is around 1700 m across track and 300 m along track. The returning echo is sampled in 128 bins each 1.563 ns resulting in a range resolution of 0.486 m.

For this study we use baseline B Level 1b (SIR_SAR_L1B) and Level 2 (SIR_SAR_L2) SAR mode data for the winter 2012/2013 (November - March). Level 1b data, containing the radar altimeter signal waveforms, can be used to retrieve quantities such as surface elevation, freeboard or thickness. Based on the waveforms in the level 1b data set we calculate the following parameters:

- *Maximum (Max)* value of the waveform power.
- *Leading Edge Width (LeW)* is obtained by fitting a cubic spline to each waveform and calculating the distance between the first bins containing a signal strength above 5% and 99% of the maximum power.
- *Trailing Edge Width (TeW)* is obtained by fitting a cubic spline to each waveform and calculating the distance between the last bins containing a signal strength above 99% and 5% of the maximum power.

Level 2 data does not yet contain information about freeboard, but contains some parameters which give information about the returned signal waveform. From the level 2 data set we analyse the following parameters:

- *Pulse Peakiness (PP)* is the ratio of the maximum power and the accumulated signal power (first defined by Laxon (1994)):

$$PP = \frac{\max(\text{power})}{\sum_{i=1}^{128} \text{power}(i)} \quad (1)$$

- *Stack Standard Deviation (SSD)* is the standard deviation of the multi-looked waveforms used at each location.
- σ_0 is the radar backscatter coefficient.

The objective of the study is to analyze waveform characteristics over sea ice, so waveforms reflected from leads are excluded from further analysis. We identify leads using the Pulse Peakiness and the Stack Standard Deviation as done previously by Laxon et al. (2013) and Hendricks

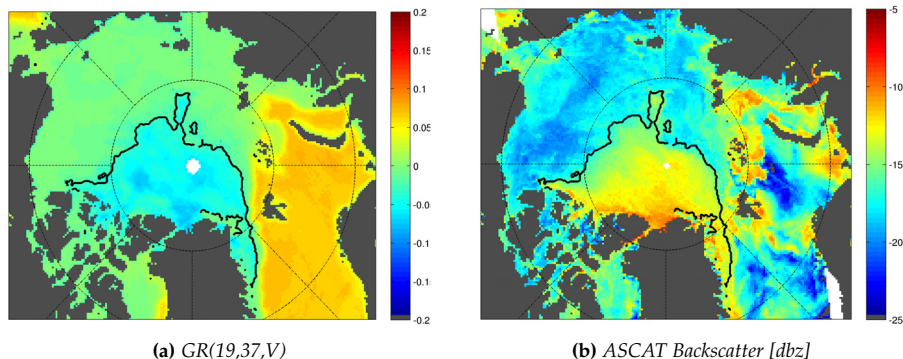


Figure 1: Spatial distribution of remote sensing retrievals used to identify sea ice type (December 2012). a) Gradient of vertically polarized 19 and 37 GHz brightness temperatures $GR(19,37,V)$. b) ASCAT σ_0 backscatter. Black contour line in both plots shows the border of First and Multi-Year-Ice (based on the OSI SAF retrieval) with Multi-Year-Ice north of Greenland.

et al. (2013). Waveforms are rejected if the Pulse Peakiness is larger than 15 or the Stack Standard Deviation smaller than 4.

All parameters are averaged and gridded to a polar stereographic projection on a 25 km grid. Outliers, defined by a distance of more than 3 standard deviations from the mean, are removed to reduce noise. So far we only use data retrieved in SAR mode. Thus a data gap occurs north of Greenland in the so-called 'Wingham Box' (see <https://earth.esa.int/web/guest/-/geographical-mode-mask-7107> for updated mode map). SARIn mode is originally designed for operations over ice caps and ice sheet margins but is also used for algorithm testing over this area of the Arctic ocean (e.g. Armitage and Davidson, 2013).

2. Other data

A. Sea ice type

For comparison we use the binary sea ice classification (First-Year-Ice vs. Multi-Year-Ice) available from the EUMETSAT Ocean and Sea Ice Satellite Application Facility (OSI SAF, www.osi-saf.org). Ice classes are based on SSMIS and ASCAT measurements, using a Bayesian approach. From SSMIS data the algorithm uses the gradient ratio of the 19 and 37 GHz vertically polarized channels $GR(19,37,V) = (Tb_{37v} - Tb_{19v}) / (Tb_{37v} + Tb_{19v})$, and from ASCAT the σ_0 backscatter. The signal from the two instruments and the resulting sea ice type is visualized in Figure 1. More information about this product can be found in Eastwood (2012) and in Breivik and Eastwood (2009). In all Figures the sea ice type is given as black contour line for each respective month.

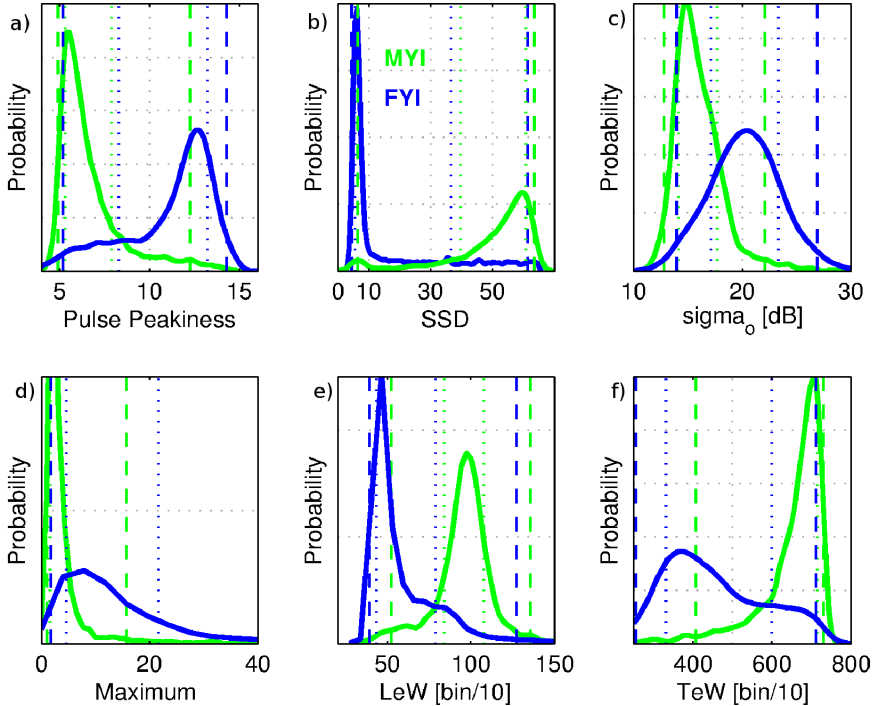


Figure 2: Probability distribution functions (PDF) for different CryoSat-2 SIRAL parameters: a) Pulse Peakiness b) Stack Standard Deviation and c) σ_{a_0} d) Maximum e) Leading Edge Width f) Trailing Edge Width. Green lines show distributions for Multi-Year-Ice (MYI) and blue lines for First-Year-Ice (FYI). Dashed and dotted lines in all 6 figures correspond to 15.9th and 84.13th percentile and 2.3th and 97.7th percentile which are the 1st and 2nd standard deviation in a normal distribution. Distributions are smoothed for visualization with gaussian kernel functions.

B. Sea ice drift

We use the low resolution sea ice drift product from the EUMETSAT Ocean and Sea Ice Satellite Application Facility (OSI SAF, www.osi-saf.org). It is a two day ice drift product, processed every day and provided as gridded data set on a 62 km polar stereographic grid. The multi-sensor data set is again based on data from ASCAT and SSMIS instruments, using a continuous Maximum-Cross-Correlation method for motion tracking. More information about the product can be found in Lavergne and Eastwood (2010) and Lavergne et al. (2010).

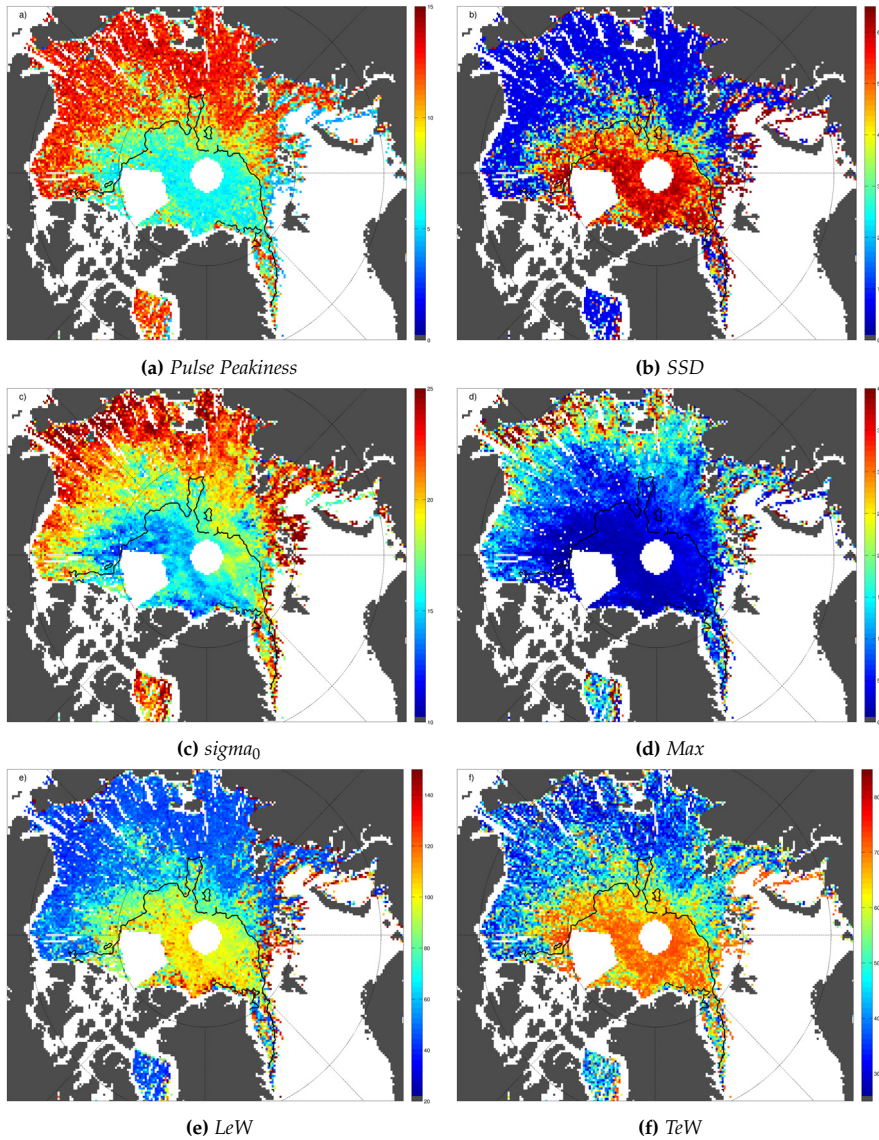


Figure 3: Spatial distribution of the different CryoSat-2 SIRAL parameters in December 2012: a) Pulse Peakiness, b) Stack Standard Deviation, c) σ_0 , d) Max, e) Leading Edge Width f) Trailing Edge Width. Black contour line shows the border of First and Multi-Year-Ice (based on the OSI SAF retrieval) with Multi-Year-Ice north of Greenland.

III. RESULTS

The probability distributions of the six analyzed parameters - Pulse Peakiness, Stack Standard Deviation, Sigma_0 , Maximum, Leading Edge Width and Trailing Edge Width - is shown in Figure 2. Distributions are calculated separately for First-Year-Ice and Multi-Year-Ice using the sea ice type retrieval from OSI SAF for classification. The PDFs are shown for December 2012 but results are similar for the other months.

For the Pulse Peakiness (Fig. 2 a) a clear difference can be found in the distributions from the two ice types, with waveforms reflected from First-Year-Ice having larger values of Pulse Peakiness than from Multi-Year-Ice. Also for the Stack Standard Deviation (Fig. 2 b) a clear difference in the distributions can be found, but waveforms reflected from First-Year-Ice have smaller values than from Multi-Year-Ice. For both parameters the distribution are not only different visually but also statistically: The null hypothesis, that measurements over First-Year-Ice and Multi-Year-Ice are from the same continuous distribution, can be rejected at 5% significance level (2 sided Kolmogorov-Smirnov test). The Leading and Trailing Edge width are larger from waveforms reflected from Multi-Year-Ice than First-Year-Ice, and show significantly different distributions over these two ice types (5% significance level) (Fig. 2 e & f). The distributions of backscatter sigma_0 are closer to each other but have a tendency towards higher values for First-Year-Ice (Fig. 2 c). The maximum of the signal waveform is larger for waveforms reflected over First-Year-Ice but the distribution from First- and Multi-Year-Ice overlap to a large extent (Fig. 2 d).

The spatial distributions of the six CryoSat-2 parameters for December 2012 are shown in Figure 3. In particular the Pulse Peakiness, Stack Standard Deviation, Leading and Trailing Edge have a similar spatial pattern. For the Pulse peakiness clearly smaller values can be found in the western part of the Arctic Ocean north of Greenland and the Canadian Archipelago, and higher values towards the southern part of the Beaufort see, the Chuckchi, Siberian and Laptev Sea. For the other three parameters Stack Standard Deviation, Leading and Trailing Edge the same pattern can be found, but higher values are observed in the western part of the Arctic Ocean. The spatial distribution of the Maximum power and the sigma_0 backscatter show a more blurry distributions (Fig. 3 c) & d)), with no clear borders between different surface regimes.

In Figure 3 we also show the border of Multi-Year-Ice and First-Year-Ice based on the sea ice type retrieval from OSI SAF. In the Beaufort Sea for all parameters a clear discrepancy can be found with respect to the border of the two expected sea ice types. To analyze this in more detail, Figure 4 shows the spatial distribution of the Pulse Peakiness for the months November 2012 until March 2013. While in autumn the largest discrepancy can be found in the Beaufort Sea, in February 2013 a difference mainly occurs north of Svalbard. In March, this pattern disappears, but the values of Pulse Peakiness from CryoSat-2 are lower in the swath from the North Pole to the East Siberian Sea than previously found over the First-Year-Ice in this region. For the other

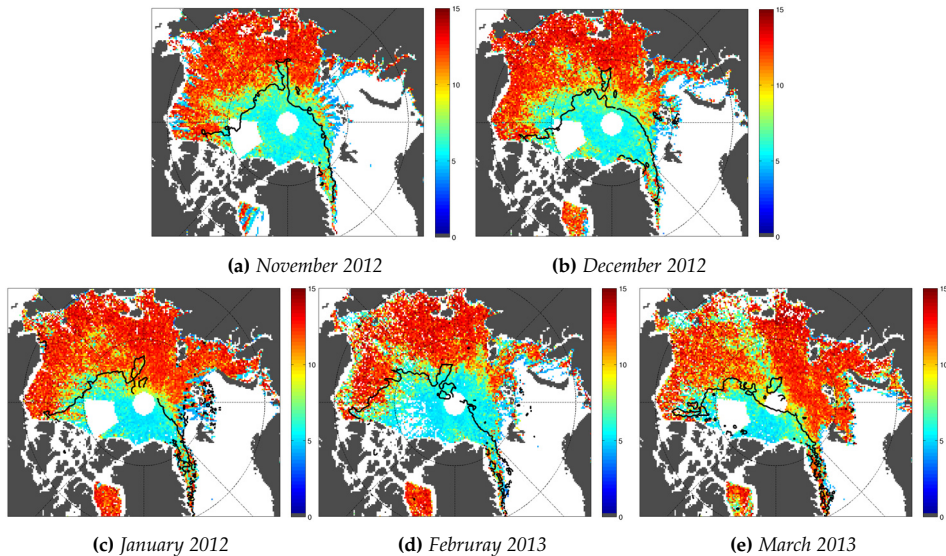


Figure 4: Spatial distribution of Pulse Peakiness for different months. Black contour line shows the border of First and Multi-Year-Ice (based on the OSI SAF retrieval) with Multi-Year-Ice north of Greenland.

parameters we found a very similar pattern for each month (not shown).

IV. DISCUSSION

We have analyzed different waveform characteristics from CryoSat’s synthetic aperture radar altimeter SIRAL over Arctic sea ice. To be able to quantify the waveform characteristics over different surface regimes we used the following parameters: Pulse Peakiness, Stack Standard Deviation and σ_0 , Maximum, Leading Edge Width and Trailing Edge Width. Below we will first discuss our findings with respect to the physical and dynamical properties of sea ice and further discuss how our results can be used in future studies.

We found a statistically significant difference between the waveform parameters Pulse Peakiness and Stack Standard Deviation, Leading Edge Width and Trailing Edge Width from the waveform signal reflected from First- and Multi-Year-Ice (Figure 2). For σ_0 the difference is not that distinct, but larger values can be found for waveforms coming from First-Year-Ice. For the power Maximum the distributions are even closer but smaller values are found for Multi-Year-Ice.

Our results are consistent with previous studies (Ulander, 1987; Fedor et al., 1989; Drinkwater,

1991; Fetterer, 1992) showing that the radar signal decreases and becomes wider from First- to Multi-Year-Ice. However, in their analysis of airborne synthetic aperture radar waveforms, Zygmuntowska et al. (2013a) concluded that the power Maximum and the Trailing Edge Width are the most suitable parameters to use for sea ice classification. In our study, based on the waveform shape from satellite based altimeters, we identified the Stack Standard Deviation, Leading Edge Width and Pulse Peakiness as the best parameters to distinguish between First- and Multi-Year-Ice. The power Maximum could not be confirmed as a reliable parameter for sea ice classification.

The spatial distribution generally shows a pattern that is consistent with the ice type retrieval from OSI SAF. However, we find discrepancies over large regions, which differ over the winter season (see Figure 4). In autumn the discrepancy is largest in the Beaufort Sea and in February 2013 it mainly occurs north of Svalbard. In March, this pattern disappears, but the values of Pulse Peakiness from CryoSat-2 are lower along the swath from the North Pole to the East Siberian Sea than previously found over the First-Year ice in this region.

To understand the inconsistencies found it is important to understand the physical properties of the surface that influence the sensors or algorithms. As shown in Figure 1 the sea ice type dataset from OSI SAF is driven by backscatter from ASCAT and brightness temperatures measured by SSMIS. For ASCAT a difference in sea ice types can be expected from a combination of dielectric properties of the surface and the roughness of the surface. Dielectric properties are dominated by relative proportions of ice, brine and air in the ice, as well as the shapes and spatial arrangements of brine and salt inclusions (Weeks, 2010). The roughness is driven by deformation and is thus often associated with the age of sea ice. For First-Year-Ice, the dielectric properties do not allow the signal to penetrate. Thus mainly surface scattering occurs and the returned signal is highly sensitive to surface roughness. Multi-Year-Ice in turn has survived one summer and is more porous and less saline. The signal can penetrate in the upper layer of the ice and so in addition to surface scattering, volume scattering also occurs. Brightness temperature from passive microwave measurements is defined by the physical temperature and the dielectric properties of the surface, as described above. The physical temperature is higher for thicker snow and thinner ice (Perovich and Elder, 2001) but it is hard to quantify a difference between ice types. However, the dependency of the brightness temperature on these properties varies for different frequencies, and the gradient between different frequencies can be used to derive information about the sea ice type (Steffen et al., 1992, also visualized in Fig. 1a) for December 2012).

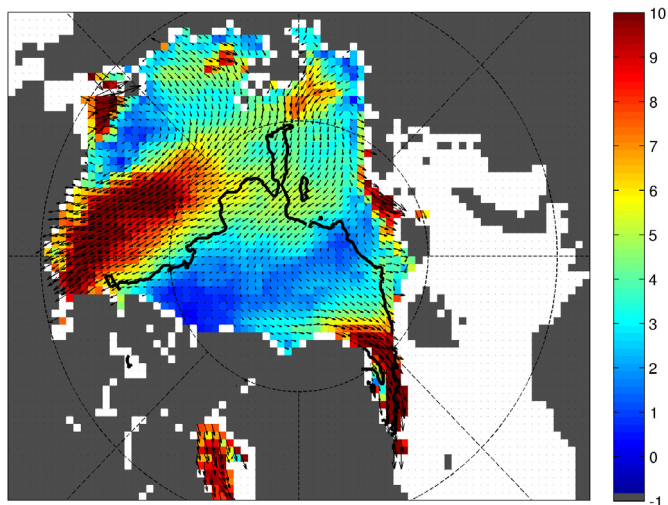
The radar signal waveform from CryoSat-2 is dependent on the properties of sea ice and snow (Fetterer, 1992). The snow properties that most influence the signal are snow depth and snow density. Besides the snow fall that determines the snow depth, the atmospheric temperature influences the snow via two different mechanisms: 1) Warm temperatures lead to melt and higher density of snow, 2) Extreme warm events, that caused surface melting followed by a freeze up, result in internal ice layers within the snow. The first effect changes the speed with which the

signal penetrates through the layer, and the second changes the scattering surface. Both effects have been found to influence significantly the scattering surface and the shape of the radar waveform (Tonboe et al., 2006), in particular the Leading Edge. From the sea ice itself no volume scattering occurs and mainly the surface roughness influences the returned signal waveform. The dependency of backscatter on surface roughness has previously been found to be non-linear and highly variable (Fetterer, 1992).

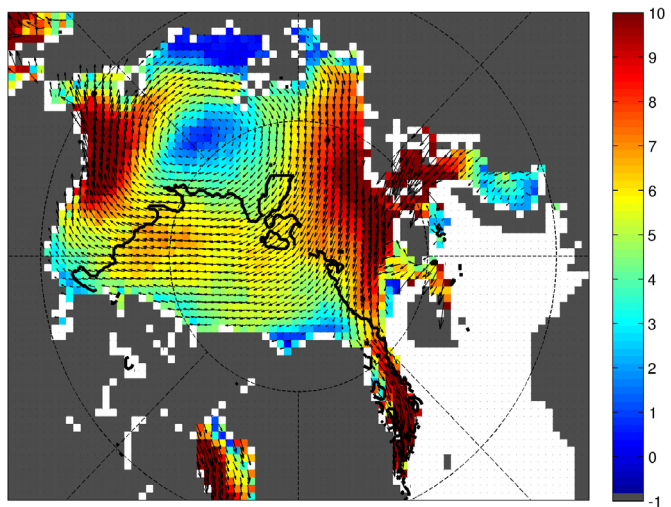
Due to a lack of data we are neither able to perform a detailed analysis of the snow properties nor the actual surface roughness. To get more information about the snow properties, we analyzed surface temperatures from ERA-Interim. We checked if the monthly mean of the daily maximum temperature and the monthly maximum vary for the regions where discrepancies occur, but did not find any anomalies (not shown). To get information about sea ice roughness we analyzed sea ice drift in different months. We found areas with values more typical for Multi-Year-Ice for the CryoSat-2 parameters over regions with First-Year-Ice, where a strong gradient in the ice drift can be observed (see Fig. 5 for examples and Figure 4). This indicates that the waveform characteristics from CryoSat's radar altimeter SIRAL are dependent on the surface 'type' but hereby meaning flat and deformed ice. As long as this surface properties go together with sea ice age (meaning First-Year-Ice and Multi-Year-Ice) a classification of these two ice types is possible. In some areas, however, this is not the case, which makes a definite classification with respect to sea ice age difficult.

The discrepancy found in the Beaufort Sea region in November occurs only over a small area. One could thus argue that the binary classification from OSI SAF provides a simplified picture, while CryoSat-2 parameters provide more details about the fraction of each ice type. However, the underlying, non-binary retrievals used for the classification from OSI SAF (see Figure 1 for December) do not resemble the spatial distribution of the CryoSat-2 parameters. Thus we can refute the hypothesis that discrepancies are only due to the difference between a binary and fractional classification (compare Figure 4 b and Figure 1 for December).

A limitation of our work is the lack of a reliable information about the sea ice type. The large scale pattern is the same for the two instruments OSI SAF is based on, but on a basin or sub basin scale quite a few discrepancies can be found. Another widely used sea ice type retrieval is the ice age retrieval developed by Fowler et al. (2004) and Maslanik et al. (2011). The retrieval is based on a completely different approach, identifying sea ice with radiometers (AVHRR, SSMIS) and tracking its movement on a weekly basis. As the method is so different, it could provide an independent evaluation. However, the distribution of sea ice age neither corresponds to ASCAT backscatter, nor the gradient from the brightness temperatures nor the different surface regimes found from CryoSat-2 parameters (comparison not shown). As the data set is based on a Lagrangian tracking approach, errors in sea ice drift may accumulate and potentially introduce large errors in the final retrieval. In our analysis we therefore use the well validated retrieval from OSI SAF as ground



(a) November 2012



(b) February 2013

Figure 5: Sea ice drift from OSI SAF for a) November, 20th 2012 and b) February, 10th 2013. Colour gives the drift 'speed' in km per two days. Black contour line in both plots shows the border of First and Multi-Year-Ice (based on the OSI SAF retrieval) with Multi-Year-Ice north of Greenland. Areas of First-Year-Ice (from OSI SAF classification) with high gradients in drift velocity correspond to areas with values typical for Multi-Year-ice for the CryoSat-2 parameters shown in Figure 3. In a) this is particularly the case in the Beaufort Sea and in b) north of Svalbard.

truth, and believe, that, on large scales, this is currently the best available product.

Our findings regarding sea ice type and roughness could be evaluated using SAR images. SAR images are limited in their coverage over the Arctic ocean, but when available, they can provide information about ice type and deformation. The SAR signal is highly sensitive to the dielectric properties of sea ice, as described for ASCAT, and deformation and roughness are well captured due to its high resolution.

The information about surface roughness based on the radar signal waveform is a valuable piece of information in itself. Above all, it can be used to reduce biases in current freeboard retrievals. The current 'operational' algorithms (Ridout et al., 2013; Hendricks et al., 2013; Laxon et al., 2013) use fixed thresholds to derive the position along the leading edge corresponding to the surface elevation. The use of a fixed threshold, however, can generate a positive bias for the freeboard retrieval, since with increasing roughness, the selected threshold should be closer to the waveform peak. This theoretical argument has been recently confirmed by Kurtz et al. (2014). They found a positive bias of almost 45 cm using freeboard estimates from a fixed threshold re-tracker compared to estimates based on an empirical model for re-tracking that takes into account for surface roughness, incidence angle and backscatter coefficient. Hendricks et al. (2013) found indeed a positive bias comparing freeboard estimates based on a fixed re-tracker to in-situ data. They argued that this bias results from an incomplete penetration of the radar signal into the snow pack. More work is required to test these two assumptions and to improve the final freeboard estimates.

V. CONCLUSIONS

We analyze the distributions of the parameters describing the shape of altimeter waveform from CryoSat-2 and find them to be significantly different over Arctic First and Multi-Year-Ice. The parameters with the largest difference between the two ice types are the Pulse Peakiness, Stack Standard Deviation and Leading Edge Width. These waveform parameters can be used to classify First- and Multi-Year-Ice over large areas of the Arctic Ocean, but in some regions clear discrepancies occur. These regions of First-Year-Ice are co-located with areas of strong gradients in drift speed, which are associated with a high rate of deformation. We find waveform parameters typical for Multi-Year-Ice in these areas and thus conclude that the radar signal is mainly sensitive to surface roughness. The information about surface roughness from radar altimeters can potentially be used to reduce biases in the freeboard retrievals.

Acknowledgment

We would like to thank the European Space Agency for processing and providing CryoSat-2 data, the National Snow and Ice Data Center (NSIDC) for providing the brightness temperatures (used

to calculate the gradient ratio $GR(19,37,V)$ in Figure 1a), and the Brigham Young University (BYU) for providing gridded ASCAT backscatter data. We further acknowledge the EUMETSAT Ocean and Sea Ice Satellite Application Facility for providing data for sea ice type, edge and drift.

REFERENCES

- Alexandrov, V., Sandven, S., Wahlin, J., and Johannessen, O. (2010). The relation between sea ice thickness and freeboard in the Arctic. *The Cryosphere*, 4:641–661.
- Armitage, T. and Davidson, M. (2013). Using the Interferometric Capabilities of ESA CryoSat-2 Mission to Improve the Accuracy of Sea Ice Freeboard Retrievals. *IEEE Transactions on Geoscience and Remote Sensing*, 52(1):529–536.
- Breivik, L.-A. and Eastwood, S. (2009). Upgrade of the OSI SAF Sea Ice Edge and Sea Ice Type products – Introduction of ASCAT. Technical report, Norwegian Meteorological Institute.
- Drinkwater, M. (1991). Ku-Band Airborne Radar Altimeter Observations of Marginal Sea Ice During the 1984 Marginal Ice Zone Experiment. *Journal of Geophysical Research*, 96(C3):4555–4572.
- Drinkwater, M., Francis, R., Ratier, G., and Wingham, D. (2004). The European Space Agency's earth explorer mission CryoSat: measuring variability in the cryosphere. *Annals of Glaciology*, 39(1):313–320.
- Eastwood, S. (2012). Ocean & Sea Ice SAF Sea Ice Product Manual–v3.8. Technical report, EUMETSAT OSI SAF.
- Fedor, L. and Brown, G. (1982). Waveheight and wind speed measurements from the Seasat radar altimeter. *Journal of Geophysical Research: Oceans (1978–2012)*, 87(C5):3254–3260.
- Fedor, L., Hayne, G., and Walsh, E. (1989). Ice-type classifications from airborne pulse-limited radar altimeter return waveform characteristics. In *International Geoscience and Remote Sensing Symposium, 1989. IGARSS'89. 12th Canadian Symposium on Remote Sensing., 1989*, volume 3, pages 1949–1952. IEEE.
- Fetterer, F. (1992). *Microwave remote Sensing of Sea Ice*, volume 68 of *Geophysical Monograph Series*, chapter 7: Sea ice altimetry, pages 111–135. American Geophysical Union.
- Fowler, C., Emery, W., and Maslanik, J. (2004). Satellite-derived evolution of Arctic sea ice age: October 1978 to March 2003. *IEEE Geoscience and Remote Sensing Letters*, 1(2):71–74.
- Giles, K., Laxon, S., and Ridout, A. (2008). Circumpolar thinning of Arctic sea ice following the 2007 record ice extent minimum. *Geophysical Research Letters*, 35(22):L22502.
- Giles, K., Laxon, S., Wingham, D., Wallis, D., Krabill, W., Leuschen, C., McAdoo, D., Manizade, S., and Raney, R. (2007). Combined airborne laser and radar altimeter measurements over the Fram Strait in May 2002. *Remote Sensing of Environment*, 111(2-3):182–194.

- Gourrion, J., Vandemark, D., Bailey, S., Chapron, B., Gommenginger, G., Challenor, P., and Srokosz, M. (2002). A two-parameter wind speed algorithm for Ku-band altimeters. *Journal of Atmospheric and Oceanic technology*, 19(12):2030–2048.
- Hendricks, S., Ricker, R., and Helm, V. (2013). AWI CryoSat-2 Sea Ice Thickness Data Product. Technical report, Alfred Wegener Institute.
- Kurtz, N. T., Galin, N., and Studinger, M. (2014). An improved CryoSat-2 sea ice freeboard and thickness retrieval algorithm through the use of waveform fitting. *The Cryosphere Discussions*, 8(1):721–768.
- Lavergne, T. and Eastwood, S. (2010). Low Resolution Sea Ice drift Product User’s Manual –V. 1.4. Technical Report PGL LR SID - OSI 405, EUMETSAT OSI SAF.
- Lavergne, T., Eastwood, S., Teffah, Z., Schyberg, H., and Breivik, L.-A. (2010). Sea ice motion from low-resolution satellite sensors: An alternative method and its validation in the Arctic. *Journal of Geophysical Research: Oceans (1978–2012)*, 115(C10).
- Laxon, S. (1994). Sea ice altimeter processing scheme at the EODC. *International Journal of Remote Sensing*, 15(4):915–924.
- Laxon, S., Peacock, N., and Smith, D. (2003). High interannual variability of sea ice thickness in the Arctic region. *Nature*, 425(6961):947–950.
- Laxon, S. W., Giles, K. A., Ridout, A. L., Wingham, D. J., Willatt, R., Cullen, R., Kwok, R., Schweiger, A., Zhang, J., Haas, C., Hendricks, S., Krishfield, R., Kurtz, N., Farrell, S., and Davidson, M. (2013). CryoSat-2 estimates of Arctic sea ice thickness and volume. *Geophysical Research Letters*, 40(4):732–737.
- Maslanik, J., Stroeve, J., Fowler, C., and Emery, W. (2011). Distribution and trends in Arctic sea ice age through spring 2011. *Geophysical Research Letters*, 38(13):L13502.
- Perovich, D. K. and Elder, B. C. (2001). Temporal evolution of Arctic sea-ice temperature. *Annals of Glaciology*, 33(1):207–211.
- Raney, R. (1998). The delay/Doppler radar altimeter. *IEEE Transactions on Geoscience and Remote Sensing*, 36(5):1578–1588.
- Ridout, A., Ivanova, A., Tonboe, R., and E., R. (2013). D2.6: Algorithm Theoretical Basis Document (ATBDv1). Technical report, ESA; NERSC.
- Steffen, K., Key, J., Cavalieri, D. J., Comiso, J., Gloersen, P., Germain, K. S., and Rubinstein, I. (1992). *Microwave Remote Sensing of Sea Ice*, volume 68 of *Geophysical Monograph Series*, chapter 10: The estimation of geophysical parameters using passive microwave algorithms, pages 201–231. American Geophysical Union.

-
- Stocker, T. F., Dahe, Q., and Plattner, G.-K. (2013). *Climate Change 2013: The Physical Science Basis*. Intergovernmental Panel on Climate Change 2013.
- Tonboe, R., Andersen, S., and Pedersen, L. (2006). Simulation of the Ku-band Radar altimeter sea ice effective scattering surface. *Geoscience and Remote Sensing Letters, IEEE*, 3(2):237–240.
- Ulander, L. (1987). Interpretation of Seasat radar-altimeter data over sea ice using near-simultaneous SAR imagery. *International Journal of Remote Sensing*, 8(11):1679–1686.
- Wadhams, P., Tucker III, W., Krabill, W., Swift, R., Comiso, J., and Davis, N. (1992). Relationship between sea ice freeboard and draft in the Arctic Basin, and implications for ice thickness monitoring. *Journal of geophysical research*, 97(C12):20325–20.
- Weeks, W. F. (2010). *On Sea Ice*. University of Alaska Press.
- Wingham, D., Francis, C., Baker, S., Bouzinac, C., Brockley, D., Cullen, R., de Chateau-Thierry, P., Laxon, S., Mallow, U., Mavrocordatos, C., et al. (2006). CryoSat: A mission to determine the fluctuations in Earth's land and marine ice fields. *Advances in Space Research*, 37(4):841–871.
- Zygmuntowska, M., Khvorostovsky, K., Helm, V., and Sandven, S. (2013a). Waveform classification of airborne synthetic aperture radar altimeter over Arctic sea ice. *The Cryosphere*, 7(4):1315–1324.
- Zygmuntowska, M., Rampal, P., Ivanova, N., and Smedsrud, L. (2013b). Uncertainties in Arctic sea ice thickness and volume: new estimates and implications for trends. *Cryosphere Discussions*, 7(5). Revised paper accepted for publication in TC 2014.